A five-primary photostimulator suitable for studying intrinsically photosensitive retinal ganglion cell functions in humans

Dingcai Cao Department of Ophthalmology and Visual Sciences, University of Illinois at Chicago, Chicago, IL, USA

Nathaniel Nicandro Department of Ophthalmology and Visual Sciences, University of Illinois at Chicago, Chicago, IL, USA

Pablo A. Barrionuevo Department of Ophthalmology and Visual Sciences, University of Illinois at Chicago, Chicago, IL, USA

Intrinsically photosensitive retinal ganglion cells (ipRGCs) can respond to light directly through self-contained photopigment, melanopsin. IpRGCs also receive synaptic inputs from rods and cones. Thus, studying ipRGC functions requires a novel photostimulating method that can account for all of the photoreceptor inputs. Here, we introduced an inexpensive LED-based five-primary photostimulator that can control the excitations of rods, S-, M-, L-cones, and melanopsin-containing ipRGCs in humans at constant background photoreceptor excitation levels, a critical requirement for studying the adaptation behavior of ipRGCs with rod, cone, or melanopsin input. We described the theory and technical aspects (including optics, electronics, software, and calibration) of the five-primary photostimulator. Then we presented two preliminary studies using the photostimulator we have implemented to measure melanopsin-mediated pupil responses and temporal contrast sensitivity function (TCSF). The results showed that the S-cone input to pupil responses was antagonistic to the L-, M- or melanopsin inputs, consistent with an S-OFF and (L + M)-ON response property of primate ipRGCs (Dacey et al., 2005). In addition, the melanopsin-mediated TCSF had a distinctive pattern compared with L + M or S-cone mediated TCSF. Other than controlling individual photoreceptor excitation independently, the five-primary photostimulator has the flexibility in presenting stimuli modulating any combination of photoreceptor excitations, which allows researchers to study the mechanisms by which ipRGCs combine various photoreceptor inputs.

Introduction

Human outer retinas contain four types of classical photoreceptors for image forming or visual processing, including rods, short-wavelength-sensitive (S-) cones, middle-wavelength-sensitive (M-) cones, and long-wavelength-sensitive (L-) cones. At photopic light levels, rods are saturated, and visual perception is mediated by S-, M-, and L-cones. Photopic vision is typically studied using three-primary color displays such as CRTs (Brainard, Pelli, & Robson, 2002) or DLP projectors (Packer et al., 2001), based on the trichromatic colorimetric theory that states that any test light can be matched perceptually by a combination of three well-chosen lights (primaries) when the test and matching lights have equal S-, M-, and L-cone excitations. At scotopic light levels, cones are below detection threshold and only rods signal visual information. Therefore, scotopic vision research requires only one primary because any two lights can be matched perceptually by adjusting the intensity of one of the lights to equate rod excitations. However, at mesopic light levels, both rods and cones are activated. Mesopic vision research requires a photostimulating method that can separate rod and cone inputs (Zele & Cao, 2014). Traditional mesopic vision studies have used one of the three strategies to isolate rod and cone functions in normal observers. The first strategy is to compare measurements obtained during the cone plateau phase (in which only cones are sensitive) and in the fully dark-adapted phase (in which rods are more

Citation: Cao, D., Nicandro, N., & Barrionuevo, P. A. (2015). A five-primary photostimulator suitable for studying intrinsically photosensitive retinal ganglion cell functions in humans. *Journal of Vision, 15*(1):27, 1–13, http://www.journalofvision.org/content/15/1/27, doi:10.1167/15.1.27.

doi: 10.1167/15.1.27 Received August 8, 2014; published January 26, 2015 ISSN 1534-7362

sensitive than cones), following the termination of a bleaching light (Hecht & Hsia, 1945). A shortcoming of this strategy is that during the fully dark-adapted phase, fully sensitive cones may affect rod responses, possibly leading to inaccurate inferences about rod function, especially with suprathreshold tasks. The second strategy is to compare measurements obtained from foveal and parafoveal locations. The rationale is that the density of rods is high in the parafovea but there are few or no rods in the fovea (Curcio, Sloan, Kalina, & Hendrickson, 1990). Evidence has shown, however, that the temporal properties of rod vision (Raninen & Rovamo, 1986) and chromatic properties of cone vision (Moreland & Cruz, 1959) vary with retinal location, making comparisons between the fovea and parafovea results ambiguous. The third strategy is to use an adapting light (typically a long-wavelength light) to desensitize cones selectively. This strategy cannot completely isolate rod activity because, in the dark-adapted eye, rods and cones have roughly the same sensitivity at long wavelengths (Crawford & Palmer, 1985), and S- and M-cones are not completely desensitized by a long wavelength adapting light. More recently, a four-primary photostimulating method was developed that allows control of the stimulation of rod and of the three types of cones independently at the same chromaticity, retinal locus, and light level (Pokorny, Smithson, & Quinlan, 2004; Puts, Pokorny, Quinlan, & Glennie, 2005; Shapiro, Pokorny, & Smith, 1996). The four-primary photostimulator has been used to study many aspects of rod-cone interactions in mesopic vision (see review, Zele & Cao, 2014).

In addition to the classical rod and cone photoreceptors, a new type of photoreceptor, called intrinsically photosensitive retinal ganglion cells (ipRGCs), was discovered in mammalian inner retinas recently (Berson, Dunn, & Takao, 2002; Hattar, Liao, Takao, Berson, & Yau, 2002). IpRGCs express melanopsin, a photopigment that can respond to light directly (Provencio et al., 2000). In addition, ipRGCs also receive synaptic inputs from rod and cone photoreceptors (Dacey et al., 2005), possibly through conventional retinal circuitries (Altimus et al., 2010; Viney et al., 2007; Weng, Estevez, & Berson, 2013). IpRGCs project to brain areas associated with non-image-forming functions, such as the SCN for circadian photoentrainment (Hattar et al., 2003; Ruby et al., 2002) and the olivary pretectal nucleus (OPN) for controlling pupil size (Clarke, Zhang, & Gamlin, 2003; Hattar et al., 2002; Lucas et al., 2003). IpRGCs also project to the LGN (Berson, 2003; Dacey et al., 2005) and may contribute to image-forming processes (Barrionuevo & Cao, 2014; Brown et al., 2012; Horiguchi, Winawer, Dougherty, & Wandell, 2013; Zaidi et al., 2007).

The photoreceptors have different but overlapping operational ranges (Dacey et al., 2005). Rods are supposed to be active at scotopic and mesopic illuminance ranges, and cones operate at mesopic and photopic illuminance ranges (Hood & Finkelstein, 1986). Recent studies have shown that rods can contribute to the circadian system at high (photopic) illuminances through ipRGCs (Altimus et al., 2010). Melanopsin is activated at an intermediate mesopic range (i.e., melanopsin activation threshold is higher than cone activation threshold) (Barrionuevo et al., 2014; Dacey et al., 2005) and is highly resistant to light bleaching (Sexton, Golczak, Palczewski, & Van Gelder, 2012). Therefore, ipRGCs can potentially combine the inputs from S-, M-, and L-cones, rods and melanopsin at some light levels (intermediate mesopic range to low photopic range, and possibly to high photopic light levels). To study five photoreceptor inputs to ipRGCs in human retinas that contribute to the non-image-forming and image-forming functions, a new photostimulating method is required.

Here, we introduced a new LED-based five-primary photostimulating method that can independently control the excitation of melanopsin-containing ipRGC, rod and cone photoreceptors at constant background photoreceptor excitation levels. Typical behavioral or electrophysiological studies of ipRGC functions use light pulses on a dark background. Few ipRGC research studies have been done under light adapted conditions (Lucas, 2013) with an intact retina (Allen et al., 2014). The five-primary photostimulating method will provide a more naturalistic light stimulation condition and may reveal a more complete picture about interactions among various photoreceptor inputs to ipRGCs that subsequently contribute to non-image-forming or image-forming functions (Lucas, 2013). We first introduced the theory of the five-primary photostimulating method. Then we described the technical aspects (including optics, electronics, software and calibration) of the five-primary photostimulator that we have implemented. Finally, we presented two preliminary studies using the photostimulator to measure melanopsin-mediated pupillary responses and temporal contrast sensitivity function (TCSF).

Theory

The theoretical basis for achieving independent control of the activities of five types of photoreceptors (S-cones, M-cones, L-cones, rods, and melanopsin-containing ipRGCs) in the human retina using a five-primary photostimulating method is silent substitution (Estévez & Spekreijse, 1982). The five-primary photostimulating method is an extension of the four-primary

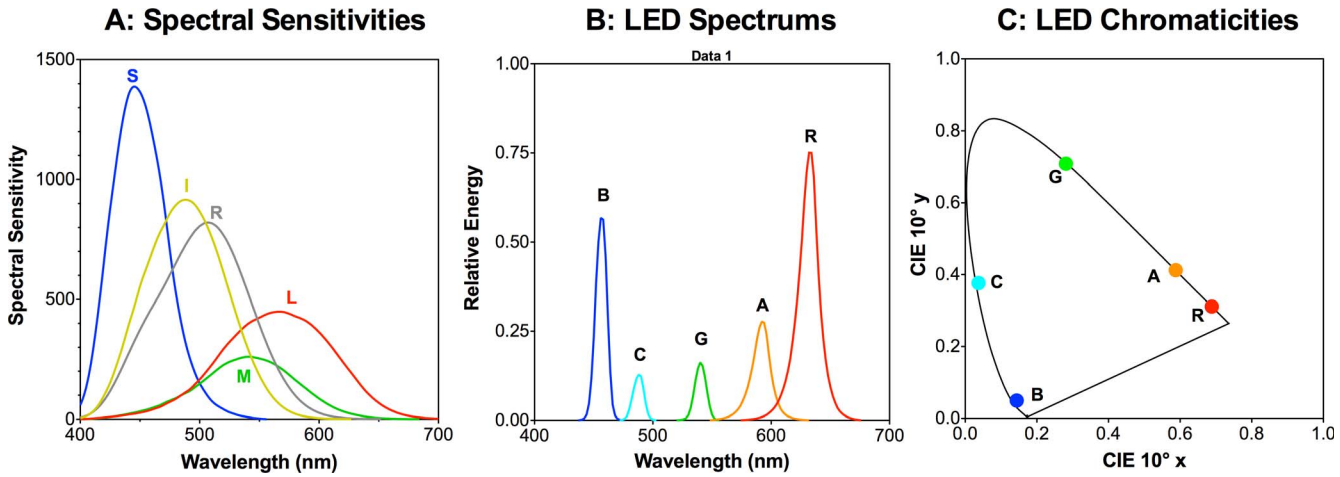

Figure 1. The relative spectral sensitivities of the five photoreceptors in human retina, including S-, M-, L-cones, rods, and ipRGCs (A), LED spectral distributions (B), and LED chromaticities in 1964 CIE 10° space (C).

photostimulating method that is used to control the stimulation of rods and the three types of cones independently (Pokorny et al., 2004; Shapiro et al., 1996). Since the details of the theoretical basis for achieving photoreceptor isolation in a four-primary photostimulator are provided by Shapiro et al. (1996), we just provided a short description of the theory here. Simply, the rod, S-, M-, L-cone spectral sensitivity functions are identical to those used in a four-primary method (Shapiro et al., 1996). The melanopsin-mediated ipRGC excitation (I) is computed according to the melanopsin spectral sensitivity function that accounts for cornea and lens spectral filtering, $\overline{mel}(\lambda)$ (al Enezi et al., 2011). The spectral sensitivity functions are normalized such that (a) photopic retinal illuminance is specified as the sum of L- and M-cone excitations; i.e., (L + M) (MacLeod & Boynton, 1979); (b) for an Equal-Energy-Spectrum (EES) light at 1 photopic Troland (Td), the S-, M-, and L-cone, rod, and melanopsin-mediated ipRGC excitations will be 0.6667 L-cone Td, 0.3333 M-cone Td, 1 S-cone Td, 1 rod Td, and 1 melanopsin Td, respectively; see Figure 1A for the photoreceptor spectral sensitivity functions (Barrionuevo & Cao, 2014; Barrionuevo et al., 2014; Cao & Barrionuevo, 2014). In other words, for an EES light, the photoreceptor excitation relative to photopic luminance is $l = \mathrm{L}/(\mathrm{L}+\mathrm{M}) = 0.6667$, $m = \mathrm{M}/(\mathrm{L}+\mathrm{M}) = 0.3333$, $s = \mathrm{S}/(\mathrm{L}+\mathrm{M}) = 1$, $r = \mathrm{R}/(\mathrm{L}+\mathrm{M}) = 1$, $i = \mathrm{I}/(\mathrm{L}+\mathrm{M}) = 1$ (Barrionuevo & Cao, 2014). Note that the L-cone chromaticity of 0.6667 for an EES light arises from the CIE XYZ normalization of EES at 1 Td to have X = 0.3333, Y = 0.3333. Since CIE Y is normalized as the luminance and the luminosity spectral sensitivity is comprised of 2:1 L:M cone contributions (Smith & Pokorny, 1975), when EES is expressed in the MacLeod-Boynton cone space, the relative L:M cone weightings at EES are 2:1 (MacLeod & Boynton, 1979). The quantification of the five photoreceptor excitations is also consistent with a current recommendation for light specification in the "melanopsin age" (Lucas et al., 2014).

For a five-primary photostimulator, suppose that the spectral distributions of the five LEDs at their maximal outputs are $\tilde{P}_1(\lambda)$, $\tilde{P}_2(\lambda)$, $\tilde{P}_3(\lambda)$, $\tilde{P}_4(\lambda)$, $\tilde{P}_5(\lambda)$, with $\alpha = [p_1\ p_2\ p_3\ p_4\ p_5]$ representing the proportion of its maximum for each LED, the photoreceptor excitations $\beta = [\mathrm{S\ M\ L\ R\ I}]$ can be computed using linear algebra $\beta = \alpha\mathrm{A}$, where A is a matrix with each row representing photoreceptor excitations at the maximum output of the i^{th} LED:

$$A = \begin{bmatrix} S_1 & M_1 & L_1 & R_1 & I_1 \\ S_2 & M_2 & L_2 & R_2 & I_2 \\ S_3 & M_3 & L_3 & R_3 & I_3 \\ S_4 & M_4 & L_4 & R_4 & I_4 \\ S_5 & M_5 & L_5 & R_5 & I_5 \end{bmatrix} \quad (1)$$

To display a light for a specific combination of five photoreceptor excitations, the unique scaling coefficient for each LED can be found as $\alpha = \beta\mathrm{A}^{-1}$. With this principle, to modulate melanopsin-mediated ipRGC excitations in a temporal square-wave, for instance, with a Weber contrast of C and constant rod and cone excitations, background and peak photoreceptor excitations, β_B and β_P, respectively, are

$$\beta_\mathrm{B} = [\mathrm{S_B M_B L_B R_B I_B}], \quad \beta_\mathrm{P} = [\mathrm{S_B M_B L_B R_B I_P}] \quad (2)$$

where $(\mathrm{I_P}\text{-}\mathrm{I_B})/\mathrm{I_B} = \mathrm{C}$. Then the proportions of LEDs relative to their maximum outputs at background and peak photoreceptor excitations (α_B and α_P) are computed as:

$$\alpha_\mathrm{B} = \beta_\mathrm{B}\mathrm{A}^{-1}, \quad \alpha_\mathrm{P} = \beta_\mathrm{P}\mathrm{A}^{-1} \quad (3)$$

When α_B and α_P are presented in a temporal order defined by a square-wave form, melanopsin-mediated ipRGC excitation can be modulated while keeping the

	LED Characteristics					Spectral characteristics	
LEDs	Model	Manufacturer	Maximum forward current (mA)	Luminous intensity @20 mA (mcd)	Interference filter used	Dominant wavelength (nm)	Half-band width (nm)
Blue	NSPB500AS	Nichia Corporation	35	11,000	Yes	456	10
Cyan	NSPE510DS	Nichia Corporation	30	5,200	Yes	488	10
Green	NSPG500DS	Nichia Corporation	35	37,700	Yes	540	10
Amber	C503B-AAS	Cree, Inc	50	15,000	No	592	17
Red	NSPR510CS	Nichia Corporation	50	5,000	No	632	17

Table 1. Primary LED characteristics.

S-, M-, L- cone, and rod excitations constant. Similarly, the stimulation of one cone type (S-, M-, or L-cones) or rods can be modulated while keeping the excitations of the remaining photoreceptor types constant. One can also modulate the excitations of two, three, or four photoreceptor types by specifying different photoreceptor excitations in β_B and β_P. In short, the five-primary photostimulator is able to present light stimuli that modulate one type of photoreceptoral excitation or any combination of photoreceptor excitations, while maintaining the same adaptational photoreceptor excitation level. This photoreceptor isolating method can be applied to the spatial domain if two lights are displayed to two different visual areas. Next, we describe the technical details of the five-primary photostimulator that we implemented.

Design

Overview

We chose LEDs as the primaries for our photostimulator. LEDs are a good choice for use as visual stimulation light sources due to their narrow-band spectral emissions and the ability to precisely control light output. The lights from five LEDs with different spectral distributions were mixed through an optical arrangement. The light outputs of the LEDs were controlled by an Arduino-based stimulation system that is inexpensive and can be easily used by those without advanced electronics skills (Teikari et al., 2012). We chose a TLC5940 chip (Texas Instruments, Dallas, TX) that allows for independent control of up to 16 channels of LEDs on a single unit with a 12-bit resolution.

Optics

The photostimulator combined lights from five bright "blue," "cyan," "green," "amber," and "red" LEDs (see Table 1 for their manufacturers and model information). To improve the instrument gamut, the "blue," "cyan," and "green" LED lights were selectively filtered with narrow-band interference filters. The spectrums and the CIE 1964 10° x, y chromaticities of the LEDs combined with the interference filters are shown in Figures 1B and 1C, respectively (also see Table 1 for the dominant wavelengths and half-band widths of their spectrums). A bundle of five optic fibers transmitted light from the LEDs through a spatial homogenizer and diffuser. A field lens placed the image of the diffuser in the plane of a 2 mm artificial pupil for a Maxwellian view (see Figure 2 for the optical layout and a picture of the photostimulator). Neutral density filters could be placed between the diffuser and the field lens to reduce light levels for all LEDs, or they could be placed in front of the LEDs to reduce light levels for individual LEDs.

LED light output control

The light output from each LED was controlled by a laboratory constructed, Arduino-based, electronic board, which consisted of a LED driver (TLC5940, ~$7 per unit) and an Arduino microcontroller (Arduino Uno SMD R3, Model A000073, ~$27 per unit). The microcontroller was connected to a MacBook Pro laptop (OS X 10.7) through a USB port.

LED driver

The TLC5940 chip had sixteen independent channels with 12-bit resolution per channel. The built-in delay between channels is 30 ns at maximum. Therefore, the maximum delay incurred from channel 1 to channel 16 is 30 ns $\times$ 15 = 0.45 μs, which is negligible when considering the temporal limits of visual processing (Felius & Swanson, 1999). The TLC5940 chip controls the LED light outputs by Pulse Width Modulation (PWM), a common dimming technique used in LED lighting. LED current is pulsed in an updating frequency f_0. A maximum current level,

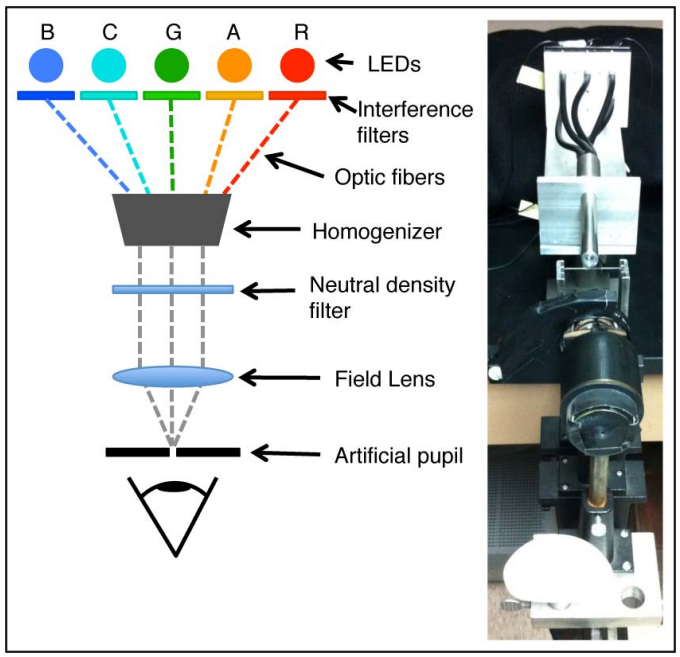

Figure 2. The optical layout and picture of the five-primary photostimulator we implemented.

I_0, is set along with the updating period, T_0, in which the LED is switched from I_0 (ON) to 0 mA (OFF) after an amount of time has passed that is dependent upon the duty cycle, D, set for the current update period. The duty cycle is defined as the percentage of ON time during T_0 so that the average current during T_0 will be proportional to D with I_0 as maximum. If T_0 is made to be smaller than 10 ms, then the modulation f_0 would be $>$ 100 Hz, leading to the average luminance to be perceived by the human eye due to temporal integration. Therefore, the light output can be modulated by changing the duty cycle and is highly linear with respect to the duty cycle.

The PWM frequency currently used was 976.5625 Hz such that the driver can represent a signal that has frequency components up to $\sim$ 488 Hz. This PWM frequency was more than sufficient for vision research since human critical fusion frequency is less than 100 Hz (Felius & Swanson, 1999; Hecht & Smith, 1936). The TLC5940 chip requires only one external resistor to set the maximum achievable current level, $I_{0,}$ for PWM dimming for all channels. For our system, we added a resistor (1 kΩ) that set the maximum achievable current level to be 39.06 mA. Additionally, the TLC5940 has the capability to independently control the current of each channel digitally without affecting the dynamic range through dot correction. This is done programmatically by setting the dot correction values of each channel to an integer in the range 0-63, where 63 signifies that the current draw for that channel is I_0. For example, if I_0 is set to 39.06 mA, but the dot correction value for a channel 1 is 40, then the maximum current for this channel will be set to $(40/63) \times I_0 = 24.8$ mA. Having this feature is very useful to reduce thermal shift in LED spectrums and reduce the turn-on transients in the LED outputs. We set the dot correction values as 43, 30, 42, 40, and 40 for the "blue," "cyan," "green," "amber," and "red" LED respectively. Figure 3A shows the dominant wavelengths of the LEDs without interference filters at 1%, 5%, 10%, 20%, 40%, 60%, 80%, and 100% of the duty cycle, measured with a PR-670 spectroradiometer (Photoresearch, Chatsworth, CA). Clearly, there were minimal thermal shifts in the dominant wavelengths (as well as CIE x, y chromaticities, not shown) for the LEDs controlled by the TLC5940 chip. Other studies (Gu, Narendran, Dong, & Wu, 2006; Muthu, Schuurmans, & Pashley, 2002) showed significant thermal shifts in LED chromaticities using a PWM dimming method, probably due to the high-power LEDs they used required about 10 times higher current level than the LEDs we used.

Microcontroller

The microcontroller that served as the intermediary between the TLC5940 and the controlling computer was the Arduino Uno SMD R3, which features an Atmel Atmega 328. Arduino (http://www.arduino.cc/) is an open source electronics platform with a USB connection to the computer, which includes the Arduino software library written in C++ to provide a higher-level view of the microcontroller's capabilities. On the computer, the Arduino can be communicated with programmatically using standard serial device protocols. For our photostimulator, we used a baud rate of 2 Mb/s, the maximum the Arduino allowed, such that the Arduino can run all of its operations in less than the update period of the TLC5940. This allowed for the LED driver to update duty cycles smoothly without any delays.

Software

We developed custom software based on a library available online for the Arduino platform (http://code.google.com/p/tlc5940arduino/) to control the TLC5940 and LED light outputs using Objective-C in Mac OS X 10.7. The library gave access to all of the features of the TLC5940 and provided all the setup required, such as setting up timers to allow for an update frequency of 976.5625 Hz for correct functioning. After the setup of the driver, the duty cycle values for the next update period were set by a function call. An example of source code in C to control LED light outputs is shown in the Appendix.

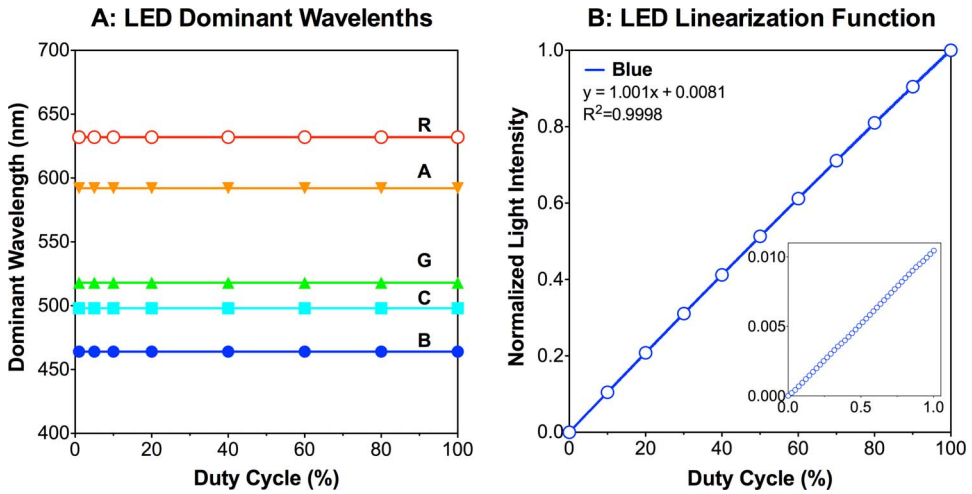

Figure 3. (A) The LED dominant wavelengths (without interference filters) at 1%, 5%, 10%, 20%, 40%, 60%, 80%, and 100% duty cycle (measured by PR 670 spectroradiometer). There are little thermal shifts in dominant wavelengths (< 1 nm) for all LEDs. (B) The normalized light intensity (measured by International Light ILT1700 in 1/4096 resolution) as a function of the duty cycle of the "blue" LED. The circles are measured light intensity at 0, 10%, 20%, 30%, 40%, 50%, 60%, 70%, 80%, 90%, and 100% of the duty cycle. The inset represents the linearization measurements for the initial 22 measurements (0%–1% duty cycle in 1/4096 resolution) to show the resolution of ILT1700. The function is highly linear, a property of PWM dimming.

Photostimulator calibration

Physical calibration

The spectral distribution of each LED combined with the interference filter was measured with the PR-670 spectroradiometer. The linearization function for each LED was obtained through radiance measurements for 4096 digital levels and for each LED with an International Light ILT1700 current meter (measurement range: 0.2 pA to 200 mA, with a resolution of 0.01 $\times$ 10_{-11} A) with a silicon detector (SED033/U, International Light Technologies, Peabody, MA). The current meter is highly linear over its large dynamic range. Figure 3B shows a highly linear light output as a function of the duty cycle for the "blue" LED, which is representative of all the other LEDs. The photopic illuminance of the "green" LED at the maximum output was measured with an EG&G 550 Radiometer/photometer (Gaithersburg, MD) and was used as a reference to calculate the illuminances of the other LEDs. The obtained photoreceptor excitations of the LEDs at their maximum output (A matrix) are shown in Table 2. The retinal illuminances for the five LEDs were 5,193 Td, 3,159 Td, 12,480 Td, 28,351 Td, and 31,509 Td (Table 2).

Observer Calibration

There are no known rhodopsin polymorphisms in human observers with normal vision (Sung, Davenport, Hennessey, Maumenee, & Jacobson, 1991); therefore, the differences in scotopic luminance sensitivity for an individual observer and the Standard Observer can be attributed to solely differences in prereceptoral filtering (Pokorny et al., 2004; Sun, Pokorny, & Smith, 2001). We conducted observer calibration by measuring individual observers' scotopic detection threshold for each LED to account for individual differences in prereceptoral filtering. The stimulus field was a 30° circular field with the central 10.5° blocked to avoid a potential artifact of spectrally selective macular pigment absorption. For each LED, observers adjusted the intensity of LED to find the minimum detectable light level. The obtained individual observer's scotopic threshold for each LED relative to the expected threshold for Standard Observer (Cao, Pokorny, & Grassi, 2011) was used to correct for individual prereceptoral filtering factor in stimulus presentation.

Photostimulator gamut

Given the A matrix of the five-primary photostimulator (Table 2), we computed the gamut of the instrument for each photoreceptor excitation modulation. For periodic (sinusoidal) stimuli, the maximal Michelson contrast of S-, M-, L-cone, rod, and melanopsin modulation was 100%, 17.3%, 22%, 18.5%, and 25.1%, respectively. Note if the interference filters were not used for "blue," "cyan," and "green" LEDs, the gamut would be reduced significantly, particularly for rod and melanopsin modulation (gamut of 7% and

LEDs	Photoreceptor excitations at LED maximum outputs (A-matrix)					Retinal illuminance (Td)
	S-cone Td	M-cone Td	L-cone Td	Rod Td	Melanopsin Td	
Blue	84,935	2,812	2,382	29,010	43,165	5,193
Cyan	4,933	1,557	1,602	10,371	13,100	3,159
Green	186	4,940	7,540	10,169	5,776	12,480
Amber	0	6,683	21,668	3,290	730	28,351
Red	0	3,587	27,922	646	94	31,509

Table 2. Photoreceptor excitations of the LEDs at their maximum outputs.

7%, respectively). For pulsed (square wave) stimuli, the Weber contrast will be at least doubled. This gamut calculation allows the background photoreceptor excitations to vary for different photoreceptor isolations. If the background photoreceptor excitations are maintained to be equal for all of the photoreceptor modulations, then the gamut (Michelson contrast) will be 100%, 17%, 22%, 17%, and 17%, respectively. Modulation with this gamut was certainly visible and it was sufficient to produce a pupillary reflex, as our preliminary study showed.

Preliminary studies using the five-primary photostimulator

We conducted two preliminary studies measuring melanopsin-based functions pupil responses (study 1) and temporal contrast sensitivity function (study 2). Both studies demonstrated that melanopsin-mediated functions are distinctive from rod- or cone- mediated functions.

Study 1: Melanopsin-mediated pupil response

We measured pupil responses for three male observers (ages between 19–44 years) with the isolated S-, M-, L-cone, rod, and melanopsin sinusoidal modulations (16% contrast, 1 Hz, mean retinal illuminance of 200 Td). The mean cone chromaticity in a relative cone Troland space of $L/(L+M) = 0.767$, $S/(L+M) = 0.12$. The stimulus field was the same as that used for observer calibration using scotopic threshold measurement (30° circular field with the central 10.5° blocked). Each observer underwent an observer calibration to correct for individual differences in pre-receptoral filtering. Observers used their right eyes to view the stimuli, and pupil sizes of their left eyes were recorded using an EyeLink II Eyetracker (SR Research Ltd, Ottawa, Ontario, Canada) at a 250 Hz sampling rate. The Arduino sent a trigger to the Eyelink II to synchronize the stimulus presentation and recording. Observers dark-adapted for 20 min followed by a 2-min light adaptation to the background light before the measurements. Then the modulations (40 s duration for each) were presented in a random order interleaved with an interstimulus interval of 30 s. The measurement was repeated three times on different days for each observer. Figure 4A shows the pupil traces (raw data) from one observer on one session with high frequency (> 1.5 Hz) and low frequency (< 0.5 Hz) components filtered out. The pupil traces indicated that the pupil was able to track the light modulation, and the S-cone induced response was approximately out of phase to that to melanopsin-induced response. The averaged pupil response amplitudes and phases derived from a Discrete Fourier Transformation for the three observers are shown in Figure 4B. Since pupil responses have high noises, we estimated the noise amplitude by averaging the amplitudes at 0.9 Hz and 1.1 Hz. The plotted response amplitude in Figure 4B represented the derived amplitude at 1 Hz after removing the noise. Clearly, the S-cone input to pupil responses was antagonistic to the L-, M-, rod, or melanopsin inputs. These results were consistent with an S-OFF and (L + M)-ON response property of primate ipRGCs (Dacey et al., 2005), an antagonistic interaction between S-cone and L-cone contributions to pupillary responses evoked by chromatic flash offset (Kimura & Young, 1999) and opponent melanopsin and S-cone signals in pupillary responses to sinusoidal stimuli (Spitschan, Jain, Brainard, & Aguirre, 2014).

Study 2: Melanopsin-mediated temporal contrast sensitivity function

Using the same stimulus configuration (30° circular field with the central 10.5° blocked), we measured temporal contrast sensitivity functions (TCSFs) for the melanopsin, cone luminance (L + M), and S-cone modulations at 2000 Td (see Figure 5). The sensitivity was determined by a 2-Yes-1-No staircase procedure. The temporal frequencies (0.25 Hz–64 Hz) were randomized. The melanopsin-mediated contrast sensitivity was not measurable for temporal frequency $\geq$

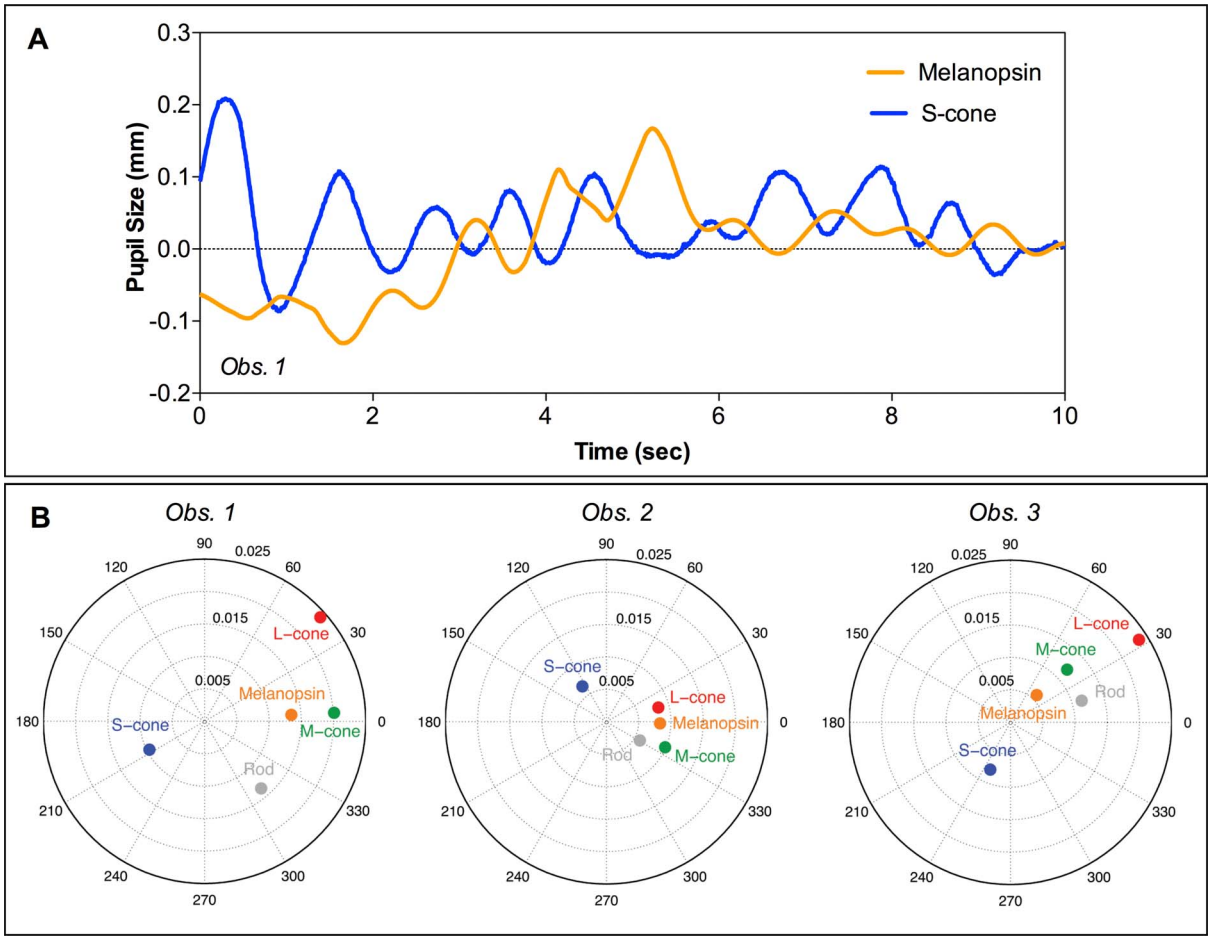

Figure 4. Pupil responses at 200 Td. (A) Representative pupil traces during the first 10 s with the S-cone (blue line) and melanopsin (yellow line) modulations (16% Michelson contrast, 200 Td) recorded during the same session from one observer (Obs. 1), after removing the steady pupil size (~4 mm). (B) Pupil response amplitudes (in mm) and phases (in degree) to the S-, M-, L-cone, rod, or melanopsin modulation at 1 Hz (16% Michelson contrast, 200 Td) for three male observers. The pupil response to the S-cone stimuli was approximately out of phase of those to the M-cone, L-cone, rod, or melanopsin stimuli.

20 Hz due to the instrument gamut. The L + M TCSF has a band-pass pattern, and S-mediated TCSF has a low-pass pattern, consistent with results from previous psychophysical studies (e.g., Burr & Morrone, 1993; Stockman, MacLeod, & DePriest, 1991; Swanson, Ueno, Smith, & Pokorny, 1987). The melanopsin-mediated TCSF, which is very different from the L + M or S-mediated TCSF, peaked at low temporal frequency (0.25–2 Hz) then reduced slightly with increasing frequency until becoming unmeasurable due to the instrument gamut. This pattern was similar to a recent finding that the melanopsin-mediated, post-illumination pupil response (PIPR, Gamlin et al., 2007; McDougal & Gamlin, 2010) was independent of temporal frequency (Joyce, Feigl, Cao, & Zele, 2015). Therefore melanopsin-mediated TCSF is relatively flat with low to intermediate temporal frequencies.

Discussion

We implemented a five-primary photostimulator based on silent substitution that can control five photoreceptor excitations independently. We reported the theory, hardware, and software aspects of the photostimulator. The Arduino-based electrical components were inexpensive, and software development to control LED light outputs was easy. Our experimental software was written in Mac OS X Objective-C, but the Arduino-based photostimulating system can be controlled by other software developing packages (see the Appendix for more details), such as Psychopy (Teikari, Malkki, Lochocki, & Hickcox, 2013), a Python-based open-source software package for handling stimulus presentation and data collection for visual psychophysics and neuroscience research (Peirce, 2007). One concern, of course, is whether the instrument gamut is

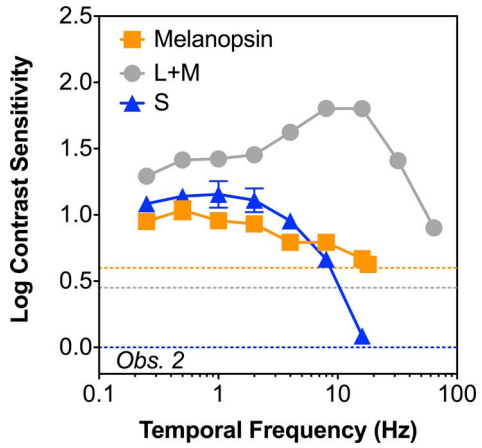

Figure 5. Temporal contrast sensitivity functions (TCSFs) for the melanopsin (orange symbols), L + M (gray symbols), or S-cone (blue symbols) modulation at 2000 Td for one observer (Obs. 2). The error bars, which are typically smaller than the symbol sizes, represent the *SEM*s from three measurements. The orange, gray, and blue dashed lines indicate the instrument gamuts for the melanopsin, L + M, and S contrast sensitivities, respectively, meaning for a specific modulation, i.e., contrast sensitivity below the dashed line is not measurable. The melanopsin-mediated contrast sensitivity is not measurable by the instrument at 20 Hz or above at this light level.

large enough for meaningful measurements of ipRGC functions with various photoreceptor inputs. As our preliminary data demonstrated, the gamut was sufficient to measure melanopsin-mediated pupil responses in the non-image-forming pathway and temporal contrast sensitivity in the image-forming pathway. In addition, our observers could all detect slight perceptual changes with the melanopsin isolating modulation at 200 Td and 2000 Td, particularly changes in brightness, as a previous study reported (Brown et al., 2012).

The advantage of the five-primary photostimulator is that it allows independent control of individual photoreceptor excitations, with constant relative photoreceptor excitations and light level, a critical requirement for study the adaptation behavior of ipRGCs with rod, cone, or melanopsin input (Do & Yau, 2013). In addition, the photostimulator can easily present stimuli modulating any combination of photoreceptor excitations, offering an opportunity to study the mechanisms by which ipRGCs combine various photoreceptor inputs for non-image-forming function or visual perception. Therefore, this five-primary photostimulator will be suitable for studying ipRGC functions in humans with normal vision (i.e., intact retinas), where noninvasive techniques are required. In principle, this device can also be used to study photoreceptor inputs to ipRGCs in nonhuman primates or other animals, as long as the photoreceptor spectral sensitivities for the species of interest are correctly estimated.

There have been several attempts by others to develop photostimulators for human ipRGC research. Viénot and associates (Viénot & Brettel, 2014; Viénot, Brettel, Dang, & Le Rohellec, 2012) developed a seven-primary system to study the rod and melanopsin inputs to pupil responses using a metameric black framework (Cohen & Kappauf, 1982; Wyszecki, 1958). They maintained cone excitations constant while searching for "black metamers" that activated both rods and melanopsin. While their experimental design did not intend to modulate rod and melanopsin excitations separately, the metameric black approach in principle can be extended to accomplish the same goal as our five-primary photostimulator. The difference is that the metameric black approach requires intensive computation to search for metameric blacks, making it difficult to generate stimuli with complex waveforms on the fly. In addition, for a seven-primary system, the solution for the metameric black is not unique with constant cone excitations. In another study (Spitschan et al., 2014), cone or melanopsin-isolating stimuli were generated in a device that allowed for the construction of arbitrary spectral power distributions digitally (OneLight Spectra, OneLight Corporation, North Vancouver, B. C., Canada). Such a device is expensive and also required an extensive search for proper spectral compositions for desired photoreceptor isolating stimuli, and the solution was not unique. In contrast, the five-primary approach we used will yield a unique solution for a certain combination of the excitations of the five types of photoreceptors. Thirdly, another group also reported developing a six-primary photostimulator to study the contribution of melanopsin to chromatic discrimination (Horiguchi et al., 2013; Horiguchi, Winawer, Wandell, & Dougherty, 2011). However, they decided not to use all of the six primaries because of the difficulty in accounting for individual variability in the transmission of the cornea and lens. Instead, they measured chromatic discrimination along many directions in the four-dimensional space defined by their four-primary lights. They found that foveal chromatic discrimination data could be modeled by trichromatic theory, but peripheral chromatic discrimination data required the involvement of the fourth pigment, potentially melanopsin (Horiguchi et al., 2013). To estimate individual prereceptoral filtering, we established an observer calibration procedure using a scotopic threshold measurement method. The procedure is fast and can be easily understood by naïve observers. The similarity of the preliminary results among three observers ranging in age from 19–44 years indicated the effectiveness of

the observer calibration. Finally, Tsujimura and colleagues (e.g., Brown et al., 2012; Tsujimura, Ukai, Ohama, Nuruki, & Yunokuchi, 2010) developed a four-primary photostimulator to study melanopsin-mediated function, assuming rods are saturated at the light levels they used. However, a four-primary method is not sufficient when rods are functioning together with melanopsin and cones.

In sum, we implemented a five-primary photostimulator that is suitable for studying ipRGC functions in humans. Using such a device may bring new insights into the mechanisms of various photoreceptor inputs to ipRGCs, which subsequently contribute to non-image-forming and image-forming processes.

Keywords: ipRGC, silent substitution, five-primary photostimulator, melanopsin, photoreceptor

Acknowledgments

This study was supported by grants from IBRO John G. Nicholls Research Fellowship (PAB), Cless Family Foundation, and UIC core grant for vision research P30-EY01792, Unrestricted Departmental Grant from the Research to Prevent Blindness. We thank Drs. Joel Pokorny and Paul Gamlin for their comments on this manuscript.

Commercial relationships: none.
Corresponding Author: Dingcai Cao.
Email: dcao98@uic.edu.
Address: Department of Ophthalmology and Visual Sciences, University of Illinois at Chicago, Chicago, IL, USA.

References

al Enezi, J., Revell, V., Brown, T., Wynne, J., Schlangen, L., & Lucas, R. J. (2011). A "melanopic" spectral efficiency function predicts the sensitivity of melanopsin photoreceptors to polychromatic lights. *Journal of Biological Rhythms, 26*(4), 314–323.

Allen, A. E., Storchi, R., Martial, F. P., Petersen, R. S., Montemurro, M. A., Brown, T. M., & Lucas, R. J. (2014). Melanopsin-driven light adaptation in mouse vision. *Current Biology, 24*(21), 2481–2490.

Altimus, C. M., Güler, A. D., Alam, N. M., Arman, A. C., Prusky, G. T., Sampath, A. P., & Hattar, S. (2010). Rod photoreceptors drive circadian photoentrainment across a wide range of light intensities. *Nature Neuroscience, 13*(9), 1107–1112.

Barrionuevo, P., & Cao, D. (2014). Rod contributions to postreceptoral pathways inferred from natural image statistics. *Journal of the Optical Society of America A, 31*(4), A131–A139.

Barrionuevo, P., Nicandro, N., McAnany, J. J., Zele, A. J., Gamlin, P. D., & Cao, D. (2014). Assessing relative rod, cone and melanopsin contributions to pupil flicker responses. *Investigative Ophthalmology and Visual Science, 55*(2), 719–727, http://www.iovs.org/content/55/2/719. [PubMed] [Article]

Berson, D. M. (2003). Strange vision: Ganglion cells as circadian photoreceptors. *TRENDS in Neurosciences, 26*(6), 314–320.

Berson, D. M., Dunn, F. A., & Takao, M. (2002). Phototransduction by retinal ganglion cells that set the circadian clock. *Science, 295*(5557), 1070–1073.

Brainard, D. H., Pelli, D. G., and Robson, T. (2002). Display characterization. In J. Hornak (Ed.), *Encyclopedia of imaging science and technology* (pp. 172–188). New York, NY: Wiley.

Brown, T. M., Tsujimura, S., Allen, A. E., Wynne, J., Bedford, R., Vickery, G., ... Lucas, R. J. (2012). Melanopsin-based brightness discrimination in mice and humans. *Current Biology, 22*(12), 1134–1141.

Burr, D. C., & Morrone, M. C. (1993). Impulse-response functions for chromatic and achromaic stimuli. *Journal of the Optical Society of America A,* (10), 1706–1713.

Cao, D., & Barrionuevo, P. (in press). Estimating photoreceptor excitations from spectral outputs of a personal light exposure measurement device. *Chronobiology International,* doi:10.3109/07420528.2014.966269.

Cao, D., Pokorny, J., & Grassi, M. A. (2011). Isolated mesopic rod and cone electroretinograms realized with a four-primary photostimulating method. *Documenta Ophthalmologica, 123,* 29–41.

Clarke, R. J., Zhang, H., & Gamlin, P. D. R. (2003). Characteristics of the pupillary light reflex in the alert rhesus monkey. *Journal of Neurophysiology, 89*(6), 3179–3189.

Cohen, J. B., & Kappauf, W. E. (1982). Metameric color stimuli, fundamental metamers, and Wyszecki's metameric blacks. *The American Journal of Psychology,* 537–564.

Crawford, B. H., & Palmer, D. A. (1985). The scotopic visibility curve and cone intrusion. *Vision Research, 25*(6), 863–866.

Curcio, C. A., Sloan, K. R., Kalina, R. E., & Hendrickson, A. E. (1990). Human photoreceptor

topography. *Journal of Comparative Neurology, 292,* 497–523.

Dacey, D. M., Liao, H., Peterson, B., Robinson, F., Smith, V. C., Pokorny, J., ... Gamlin, P. D. (2005). Melanopsin-expressing ganglion cells in primate retina signal color and irradiance and project to the LGN. *Nature,* (433), 749–754.

Do, M. T. H., & Yau, K. W. (2013). Adaptation to steady light by intrinsically photosensitive retinal ganglion cells. *Proceedings of the National Academy of Sciences, USA, 110*(18), 7470–7475.

Estévez, O., & Spekreijse, H. (1982). The "silent substitution" method in visual research. *Vision Research, 22,* 681–691.

Felius, J., & Swanson, W. H. (1999). Photopic temporal processing in retinitis pigmentosa. *Investigative Ophthalmology & Visual Science, 40*(12), 2932–2944, http://www.iovs.org/content/40/12/2932. [PubMed] [Article]

Gamlin, P. D., McDougal, D. H., Pokorny, J., Smith, V. C., Yau, K. W., & Dacey, D. M. (2007). Human and macaque pupil responses driven by melanopsin-containing retinal ganglion cells. *Vision Research,* (47), 946–954.

Gu, Y., Narendran, N., Dong, T., and Wu, H. (2006). *Spectral and luminous efficacy change of high-power LEDs under different dimming methods*. Proceedings of SPIE 6337, Sixth International Conference on Solid State Lighting, 63370J, September 12, 2006. doi:10.1117/12.680531.

Hattar, S., Liao, H. W., Takao, M., Berson, D. M., & Yau, K. W. (2002). Melanopsin-containing retinal ganglion cells: Architecture, projections, and intrinsic photosensitivity. *Science, 295,* 1065–1070.

Hattar, S., Lucas, R. J., Mrosovsky, N., Thompson, S., Douglas, R. H., Hankins, M. W., ... Foster, R. G. (2003). Melanopsin and rod–cone photoreceptive systems account for all major accessory visual functions in mice. *Nature, 424*(6944), 75–81.

Hecht, S., & Hsia, Y. (1945). Dark adaptation following light adaptation to red and white lights. *Journal of the Optical Society of America, 35,* 261–267.

Hecht, S., & Smith, E. L. (1936). Intermittent stimulation by light. IV. Area and the relation between critical frequency and intensity. *Journal of General Physiology, 19,* 979–991.

Hood, D. C., & Finkelstein, M. A. (1986). Sensitivity to Light. In K. R. Boff, L. Kaufman & J. P. Thomas (Eds.), *Handbook of Perception and Human Performance, Vol I: Sensory Processes and Perception* (Vol. 1. pp. 5-1–5-66). New York: John Wiley & Sons.

Horiguchi, H., Winawer, J., Dougherty, R. F., & Wandell, B. A. (2013). Human trichromacy revisited. *Proceedings of the National Academy of Sciences, USA, 110*(3), E260–E269.

Horiguchi, H., Winawer, J., Wandell, B. A., & Dougherty, R. F. (2011). Novel MR safe stimulator with six color channels at accurate high temporal frequencies. *Journal of Vision, 11*(11): 1236, http://www.journalofvision.org/content/11/11/1236, doi: 10.1167/11.11.1236. [Abstract]

Joyce, D. S., Feigl, B., Cao, D., & Zele, A. J. (2015). Temporal characteristics of melanopsin inputs to the human pupil light reflex. *Vision Research, 107,* 58–66.

Kimura, E., & Young, R. S. (1999). S-cone contribution to pupillary responses evoked by chromatic flash offset. *Vision Research, 39,* 1189–1197.

Lucas, R. J. (2013). Mammalian inner retinal photoreception. *Current Biology, 23*(3), R125–R133.

Lucas, R. J., Hattar, S., Takao, M., Berson, D. M., Foster, R. G., & Yau, K.-W. (2003). Diminished pupillary light reflex at high irradiances in melanopsin-knockout mice. *Science, 299*(5604), 245–247.

Lucas, R. J., Peirson, S. N., Berson, D. M., Brown, T. M., Cooper, H. M., Czeisler, C. A., ... O'Hagan, J. B. (2014). Measuring and using light in the melanopsin age. *Trends in Neurosciences, 37*(1), 1–9.

MacLeod, D. I. A., & Boynton, R. M. (1979). Chromaticity diagram showing cone excitation by stimuli of equal luminance. *Journal of the Optical Society of America, 69,* 1183–1185.

McDougal, D. H., & Gamlin, P. D. (2010). The influence of intrinsically-photosensitive retinal ganglion cells on the spectral sensitivity and response dynamics of the human pupillary light reflex. *Vision Research, 50*(1), 72–87.

Moreland, J. D., & Cruz, A. (1959). Colour perception with the peripheral retina. *Optica Acta, 6,* 117–151.

Muthu, S., Schuurmans, F. J., & Pashley, M. D. (2002). *Red, green, and blue LED based white light generation: issues and control*. Presented at the Industry Applications Conference, October 13–18, 2002, Pittsburgh, PA.

Packer, O., Diller, L. C., Verweij, J., Lee, B. B., Pokorny, J., Williams, D. R., ... Brainard, D. H. (2001). Characterization and use of a digital light projector for vision research. *Vision Research, 41*(4), 427–439.

Peirce, J. W. (2007). PsychoPy—psychophysics software in Python. *Journal of Neuroscience Methods, 162*(1), 8–13.

Pokorny, J., Smithson, H., & Quinlan, J. (2004). Photostimulator allowing independent control of rods and the three cone types. *Visual Neuroscience, 21,* 263–267.

Provencio, I., Rodriguez, I. R., Jiang, G., Hayes, W. P., Moreira, E. F., & Rollag, M. D. (2000). A novel human opsin in the inner retina. *The Journal of Neuroscience, 20*(2), 600–605.

Puts, M. J. H., Pokorny, J., Quinlan, J., & Glennie, L. (2005). Audiophile hardware in vision science; the soundcard as a digital to analog converter. *Journal of Neuroscience Methods, 142*(1), 77–81.

Raninen, A., & Rovamo, J. (1986). Perimetry of critical flicker frequency in human rod and cone vision. *Vision Research, 26*(8), 1249–1255.

Ruby, N. F., Brennan, T. J., Xie, X., Cao, V., Franken, P., Heller, C. H., & O'Hara, B. F. (2002). Role of melanopsin in circadian responses to light. *Science, 298*(5601), 2211–2213.

Sexton, T. J., Golczak, M., Palczewski, K., & Van Gelder, R. N. (2012). Melanopsin is highly resistant to light and chemical bleaching in vivo. *Journal of Biological Chemistry, 287*(25), 20888–20897.

Shapiro, A. G., Pokorny, J., & Smith, V. C. (1996). Cone-rod receptor spaces, with illustrations that use CRT phosphor and light-emitting-diode spectra. *Journal of the Optical Society of America A, 13,* 2319–2328.

Smith, V. C., & Pokorny, J. (1975). Spectral sensitivity of the foveal cone photopigments between 400 and 500 nm. *Vision Research, 15,* 161–171.

Spitschan, M., Jain, S., Brainard, D. H., & Aguirre, G. K. (2014). Opponent melanopsin and S-cone signals in the human pupillary light response. *Proceeding of the National Academy of Sciences, USA, 111*(43), 15568–15572.

Stockman, A., MacLeod, D. I. A., & DePriest, D. D. (1991). The temporal properties of the human short-wave photoreceptors and their associated pathways. *Vision Research, 31*(2), 189–208.

Sun, H., Pokorny, J., & Smith, V. C. (2001). Control of the modulation of human photoreceptors. *Color Research and Application, 26,* S69–S75.

Sung, C. H., Davenport, C. M., Hennessey, J. C., Maumenee, I. H., Jacobson, S. G., Heckenlively, J. R., et al. (1991). Rhodopsin mutations in autosomal dominant retinitis pigmentosa. *Proceedings of the National Academy of Sciences, USA, 88*(15), 6481–6485.

Swanson, W. H., Ueno, T., Smith, V. C., & Pokorny, J. (1987). Temporal modulation sensitivity and pulse detection thresholds for chromatic and luminance perturbations. *Journal of the Optical Society of America A, 4,* 1992–2005.

Teikari, P., Malkki, H., Lochocki, B., & Hickcox, K. S. (2013). Arduino-based LED stimulator system for vision research. *Journal of Vision, 13*(15): P20, http://www.journalofvision.org/content/13/15/P20, doi:10.1167/13.15.55. [Abstract]

Teikari, P., Najjar, R. P., Malkki, H., Knoblauch, K., Dumortier, D., Gronfier, C., & Cooper, H. M. (2012). An inexpensive Arduino-based LED stimulator system for vision research. *Journal of Neuroscience Methods, 211*(2), 227–236.

Tsujimura, S., Ukai, K., Ohama, D., Nuruki, A., & Yunokuchi, K. (2010). Contribution of human melanopsin retinal ganglion cells to steady-state pupil responses. *Proceedings of the Royal Society B: Biological Sciences, 277,* 2485–2492.

Viénot, F., & Brettel, H. (2014). The Verriest Lecture: Visual properties of metameric blacks beyond cone vision. *JOSA A, 31*(4), A38–A46.

Viénot, F., Brettel, H., Dang, T., & Le Rohellec, J. (2012). Domain of metamers exciting intrinsically photosensitive retinal ganglion cells (ipRGCs) and rods. *Journal of the Optical Society of America, A, 29*(2), A366–A376.

Viney, T., Balint, K., Hillier, D., Siegert, S., Boldogkoi, Z., Enquist, L., ... Roska, B. (2007). Local retinal circuits of melanopsin-containing ganglion cells identified by transsynaptic viral tracing. *Current Biology, 17,* 981–988.

Weng, S., Estevez, M. E., & Berson, D. M. (2013). Mouse ganglion-cell photoreceptors are driven by the most sensitive rod pathway and by both types of cones. *PLoS One, 8*(6), e66480.

Wyszecki, G. (1958). Evaluation of metameric colors. *Journal of the Optical Society of America, 48*(7), 451–452.

Zaidi, F. H., Hull, J. T., Peirson, S. N., Wulff, K., Aeschbach, D., Gooley, J. J., ... Czeisler, C. A. (2007). Short-wavelength light sensitivity of circadian, pupillary, and visual awareness in humans lacking an outer retina. *Current Biology, 17*(24), 2122–2128.

Zele, A. J., & Cao, D. (2014). Vision under mesopic and scotopic illumination. *Frontiers in Psychology, 5*: 1594, doi:10.3389/fpsyg.2014.01594.

Appendix

The source code in C to control LED light outputs

The software implementation for the computer was written in C for POSIX compliant operating systems. Most Unix-based operating systems are POSIX compliant but there is a small problem that must be considered when connecting to the Arduino from the computer; for the LED driver to run smoothly, the baud rate must be set higher than standard baud rates which means that the OS must provide a way to set the baud rate to a nonstandard one. This should be possible on modern operating systems.

The C program provides an interface to update the duty cycle values of the LED driver. This is done by allowing the user to provide a function that is called when those values need to be sent to the LED driver for the next update period. The user function is called repeatedly to obtain those values and send them to the Arduino. Since the program is written in C, it can be adapted to any programming language that supports calls to C code or extensions written in C; these include Python, Ruby, C++, Objective-C, and others. We developed our experimental software in Objective-C, which is essentially a superset of C in MAC OS X, so there was minimal effort in incorporating the C program into applications written in Objective-C.

An example user function is provided below that produces a square wave on all channels with a period of $2 \cdot (500 \cdot T_0)$ seconds:

```
void update_channels(int nchannel,
double count,
 float values[ ] )
{
int i;
float val;
if((int)count % 500)
val = 15.0;
else
val = 0;
for(i = 0; i < nchannel; i++)
values[ i] = val;
}
```

The user function is provided with the number of channels that are available (with a single TLC5940, this will be 16 channels), the count that represents the current update period, and lastly the array of duty cycle values (given in mA) of each channel for the specified count. The actual time of the update will be $\text{count} \cdot T_0$ seconds after the stimulus start. The function updates the LED channels by updating the values array that is specified in mA of current for each channel and is converted to duty cycle values internally.